# Characterizing drilling-induced fractures with multicomponent induction and acoustic data

Tsili Wang, Baker Atlas, U.S.A.,Berthold Kriegshäuser, Baker Atlas, Brazil, Xiaoming Tang, Liming Yu, Otto Fanini, Baker Atlas, U.S.A.,Gustavo Ugueto, Shell Exploration and Production



This paper was prepared for presentation at the 8th International Congress of The Brazilian Geophysical Society held in Rio de Janeiro, Brazil, 14-18 September 2003.



## Abstract

Drilling-induced fractures are closely related to formation stress, a critical factor for wellbore stability, completion decisions, and well planning. In this paper, we combine a crossed-dipole acoustic log with a multicomponent induction log to jointly interpret drilling-induced fractures. The joint interpretation provides information that neither log can provide separately. First, the resistivity and the acoustic logs respond differently to fractures and formation stress. The acoustic log responds to both formation stress and fractures but the induction log responds only to fractures. The resistivity log thus helps identify the existence of fractures. Second, the crossed-dipole acoustic and the induction logs have different depths of investigation. For the sensor spacings and frequencies considered for this study, the resistivity data usually have larger depths of investigation than the crossed-dipole acoustic data. This allows us to better define the depth of a drilling-induced fracture. Third, the crossed-dipole acoustic log can provide accurate information about the fracture azimuth. The fracture azimuth information is needed to estimate the fracture length. We show with a deepwater Gulf of Mexico data set the above advantages of jointly interpreting the multicomponent induction and acoustic logs for drilling-induced fractures.

## Introduction

Heavy drilling mud often induces fractures, particularly in soft formations such as deepwater shales (Aadnoy and Bell, 1998). Such fractures tend to propagate perpendicularly to the minimum horizontal stress direction. Fracture characterization based on wireline logs has been attempted in the past (Peters and Hartley, 1984). One approach to measuring fracture length involved pumping cold fluid into the fracture before and after fracturing. The fracture height is detected by interpreting the measured temperature variations and thermal decay measurements. Another approach for fracture study utilized image data analysis (Ma et al., 1993). These methods suffer from a shallow depth of investigation.

As a new approach, we combine multicomponent acoustic and the newly available multicomponent induction (Kriegshäuser et al., 2000) logs for fracture characterization. The two types of logs, when interpreted jointly, can provide information about drilling-induced fractures that neither log can provide separately.

Acoustic, particularly, crossed-dipole, measurements have been used over the past few years to detect and characterize in-situ formation stress and drilling induced fractures (e.g., Joyce et al., 1998). Such measurements provide quantitative information about the azimuth of stress and factures. Estimation of fracture depths, however, has not been attempted yet.

A multicomponent induction resistivity log has azimuthal sensitivity provided by the co-planar and cross-component measurements (Kriegshäuser et al., 2000). The azimuthal sensitivity makes possible the detection of vertical or sub-vertical drilling-induced fractures. Traditional induction tool data, however, do not have such capability.

Crossed-dipole acoustic and multicomponent induction logs respond differently to fractures and in-situ formation stress, two related but distinct features. The acoustic measurements respond to both formation stress and fractures. The induction measurements, however, respond only to fractures (not stress). A combination of the logs helps differentiate drilling-induced fractures from stress.

In this paper, we illustrate logs from a deepwater Gulf of Mexico well showing the characteristics of drilling-induced fractures. With the information provided by multicomponent induction, acoustic, and other logs, we attempt to estimate the depths of the fractures. To do so, we first study the induction response to a drilling-induced fracture using an advanced 3-D numerical simulation technique (Wang and Fang, 2001). The measured data are then matched to the fracture model data. In comparing the measured data with the synthetic data, we found that the fractures propagate about 2 ft from the borehole wall within the depth intervals of interest.

## Induction and acoustic responses to drilling-induced fractures

In hydrocarbon basins, the maximum stress is often in the vertical direction and the minimum stress is in the

horizontal direction. For this reason the fracture tends to be vertical and follows the direction of the maximum stress. Previous investigations have suggested that, except in very shallow wells, most hydraulically created fractures will be vertical (Hubbert, 1956) or nearly vertical. The fractures change the formation's mechanical and electrical properties and thus influence both acoustic and induction resistivity logs.

**Crossed-dipole acoustic response.** When a fracture traverses a borehole, crossed dipole receiver arrays will read differently, depending on the tool's azimuth relative to the fracture strike. It is sufficient to consider the special case where the transmitter and receiver dipoles are aligned either parallel or perpendicular to the fracture strike. Measurements at any other angles can be rotated to correspond to this special case (Joyce et al., 1998), provided that a full set of crossed-dipole measurements is available. If the transmitter dipole is parallel to the strike of the fracture, the flexural wave motion of the formation will be little affected by the fracture because the particle motion is parallel to the fracture plane and the fracture is connected acoustically in parallel to the formation. This results in a fast shear wave. In contrast, when the transmitter dipole is perpendicular to the fracture strike, the particle motion will traverse the fracture. In other words, the fracture is in serial connection with the formation, yielding a slow shear wave. Therefore, the polarization of the fast shear wave defines the fracture strike (Tang et al, 2000). This strike direction often corresponds to the maximum horizontal in-situ stress direction.

**Multicomponent induction response.** The induction tool considered measures XX, YY, and ZZ responses, in addition to two cross-component responses. Here, the XX data were acquired with an x-directed (perpendicular to the tool axis) transmitter coil and an x-directed receiver coil as, similarly, are the YY and ZZ data. The operating frequencies are in the range of kilohertz. For more details about the tool configuration, the reader is referred to Kriegshäuser et al. (2000). The different transmitter and receiver configurations respond differently to a drilling induced fracture. Consider a wing-like fracture in the x-direction (Figure 1). Assume the fracture is filled with resistive fluids. As Anderson et al. (1996) and Wang et al. (2001) have shown, the fracture generally reduces the ZZ apparent conductivity. Such a fracture will have almost no effect on the YY measurement but can significantly increase the XX apparent conductivity. A fracture filled with conductive mud, however, will have little effect on the ZZ and XX measurements and reduces the YY apparent conductivity.

Using a 3-D modeling algorithm (Wang and Fang, 2001), we were able to analyze the sensitivities of the XX, YY, and ZZ measurements to the fracture length. The results are shown in Figure 2. The formation is 1 Ohm-m. The mud is 1000 ohm-m. The borehole is 12 in. in diameter. The fracture aperture is 1 in. We observe that the ZZ, XX, and YY measurements have different sensitivities to the fracture length. For shallow fractures less than 2 ft in length, the ZZ measurement has almost no sensitivity. Beyond that point, the ZZ apparent conductivity decreases as the fracture length increases. The magnitude of the variation is about 200 mS/m for fractures up to 5 ft long.

Next, we examine the XX and YY responses. First, the YY measurement has no sensitivity to the resistive fracture. This result is expected because the induced current in the formation flows parallel to the fracture plane and the fracture is transparent to the induction current induced by a *y*-directed coil. However, the XX apparent conductivity increases almost linearly with the fracture length for the first 2 ft. Beyond that, the XX measurement reaches an asymptotic value. For all frequencies investigated, the XX apparent conductivity changes by about 700 mS/m, a value much greater than that for the ZZ measurement. This shows that the XX measurement has greater sensitivity to the fracture length than the ZZ measurement.

The calculated tool responses will be used later to estimate the fracture length in a Gulf of Mexico well.

**Field example**

The well is located in the Ursa field, Mississippi Canyon Block 809 about 130 miles south of New Orleans in the deepwater Gulf of Mexico. The field is within an intra-slope, salt-bound sub-basin nearly 26 miles downdip of the current shelf-slope break. The water depth is about 3800 ft. Pay zones in the Ursa field range from 12,000 ft subsea to 19,000+ ft subsea. The reservoir rocks are typically comprised of turbidite sands. The interval of interest contains a thinly laminated, low-resisitivity pay section (Mollison et al., 2001).

Figure 3 shows the XX, YY, and ZZ apparent conductivities and several other logs. The upper section (above X460 ft) contains sands and sand/shale lamination. The lower section consists mainly of shales. Note that above X460 ft, the XX and YY are almost identical. Below X470 ft, the two logs read differently over much of the interval. The maximum differences occur between X510 and X560 ft. In contrast, the ZZ log in that interval shows little variation. Meanwhile, around X530 ft, the caliper reads about 2 in. larger. The density drops by about 0.18 gm/cc between X510-540 ft, and the neutron porosity increases from about 24 pu to about 44–48 pu around X525 ft.

Figure 4 shows the differences between these XX and YY apparent conductivities. Also shown in this figure is the azimuthal shear-wave velocity anisotropy ratio derived from the cross-dipole acoustic logs. Notice the remarkable correspondence between the induction log (XX and YY) difference and the shear velocity anisotropy ratio over the log interval.

Several scenarios can cause the XX log to be different from the YY. These include (1) a deviated borehole, (2) a tilted formation, (3) cross bedding, (4) a decentralized

tool, and (5) vertical and subvertical fractures. In the depth interval of interest, the borehole dip is about 25°. The formation is nearly horizontal, dipping at about 11° to the ENE. With such a small borehole deviation and formation bedding dip, the XX and YY logs are expected to be similar. In fact, even for the upper portion (above X460 ft), which is highly laminated, the XX and YY logs are similar. Therefore, the borehole deviation and formation tilting effects are negligible. Cross bedding is unlikely because the interval consists of shales, whereas cross bedding is more typical of coarser sediments such as sands. Case (4) is eliminated because the tool was centralized. Therefore, the most likely cause for the significant differences between the XX and the YY logs is fractures.

The study of the Stoneley-wave log yields interesting observations. The Stoneley wave is an interface wave and is extremely sensitive to fluid-flow conduits (e.g., fractures) at the borehole. Figure 5 shows the Stoneley waveforms and the formation permeability derived from the Stoneley waves (Tang et al., 1998). Note that the permeability at around X525 ft depth is about two orders of magnitude higher than that found in the upper portion containing porous sands. Such an anomalously high permeability in shales indicates the existence of fractures.

The crossed-dipole acoustic logs in Figure 6 show significant shear wave splitting below X450 ft with the maximum level of splitting occurring between X500 ft and X550 ft. The azimuthal anisotropy ratio derived from the fast and slow shear waves reaches 14% around the X525 ft depth. The fast shear wave polarization direction, given in the last track of Figure 6, defines the strike direction of the fracture.

It is important to observe that the strike of the fracture remains substantially stable at around 30° from the north between X500 and X550 ft. The stable strike direction over a relatively large depth interval is consistent with the geometry of drilling-induced fractures.

**Estimation of fracture length**

We seek to estimate the fracture length with the multicomponent induction logs. In reality, the tool may be rotated in the borehole. Assume that the x-directed transmitter is at an angle θ to the *x*-axis. Then the XX and YY responses can be calculated from those shown in Figure 2 as

$$XX = XX_0 \cos^2(\theta) + YY_0 \sin^2(\theta)$$

$$YY = XX_0 \sin^2(\theta) + YY_0 \cos^2(\theta)$$

where $XX_0$ and $YY_0$ are the tool responses for θ=0 given in Figure 2.

We estimate the fracture length in the depth interval of X535-X550 ft. The angle θ in that interval is about 30°. Figure 7 shows the differences between the measured XX and YY apparent conductivities superimposed on numerically simulated data. The measured logs are selected to correspond to the maximum differences between the XX and YY logs. From Figure 7, we infer that the fracture length is about 1.5–2 ft. This relatively small fracture length seems consistent with the field observation that no massive lost circulation was observed during drilling.

**Conclusions**

Multicomponent induction and crossed-dipole acoustic logs complement each other in interpreting drilling-induced fractures. The multicomponent induction, acoustic, and other logs collected in a Gulf of Mexico well show close correspondence to the drilling-induced fractures in a shale zone. Using the fracture azimuth information derived from the crossed-dipole acoustic logs, we were able to estimate the fracture length. The estimated fracture length of 1.5-2 ft appears consistent with the field observation.

**Acknowledgments**

We are grateful to Shell for the use of the field data. We thank Baker Atlas for permission to publish this paper.

**References**

Aadnoy, B., and Bell, S., 1998, Classification of drilling-induced fractures and their relationship to in-situ stress directions: Petrophysics, **39**, 27-42.

Anderson, B., Barber, T., Druskin, V., Lee, P., and Dussan, E., 1996, The response of multiarray induction tools in highly dipping formations with invasion and in arbitrarily 3D geometries: paper A, 37th SPWLA Ann. Logging Symp.

Hubbert, M. K., Willis, D. G., 1956, Mechanics of hydraulic Fracturing, SPE Fall Meeting, Los Angeles, October 14-17.

Joyce, B., Patterson, D., and Thomas, J., 1998, Advanced interpretation of fractured carbonate reservoirs using four-component cross-dipole analysis: paper R, SPWLA 39th Ann. Logging Symp. Trans.

Kriegshäuser, B., Fanini, O., Forgang, S., Itskovich, G., Rabinovich, M., Tabarovsky, L., Yu, L., Epov, M., and v.d. Horst, J., 2000, A new multicomponent induction logging tool to resolve anisotropic formations: paper D, SPWLA 40th Ann. Logging Symp. Trans.

Ma, T. A., Lincecum, V., Reinmiller, R., Mattner, J., 1993, Natural and Induced fractures classification using image analysis: paper J, SPWLA 34nd Ann. Logging Symp. Trans.

Mollison, R.A., Fanini, O., Kriegshauser, B., Yu, L., and Ugueto, G., 2001, Impact of multicomponent induction technology on a deepwater turbidite sand hydrocarbon saturation evaluation: paper T, SPWLA 42nd Ann. Logging Symp. Trans.

Peeters, M., and Hartley, R., 1984, Induced fracture height detection from wireline logs: paper GGG, SPWLA 25th Ann. Logging Symp. Trans.

Tang, X., Altundbay, M., and Shorey, D., 1998, Joint interpretation of formation permeability from wireline acoustic, NMR, and image log data: paper KK, SPWLA 39th Ann. Logging Symp. Trans.

Tang, X., Patterson, D., Markovic, M., 2000, Fracture measurements in open/cased holes using cross-dipole logging: Theory and field results, Exp. Abstracts, 70th SEG Annual Mtg.

Wang, T., Yu, L, Kriegshäuser, B., Fanini, Otto, Merchant, A., 2001, Understanging multicomponent induction logs in a 3-D borehole environment: paper GG, SPWLA 41st Ann. Logging Symp. Trans.

Wang, T., and Fang, S., 2001, 3-D electromagnetic anisotropy modeling using finite differences: Geophysics, **66**, 1386-1398.

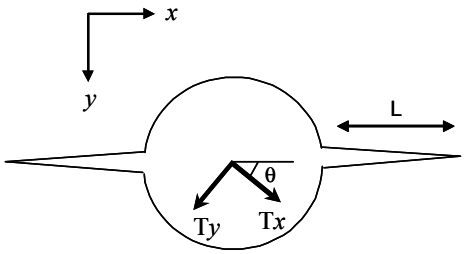


Figure 1. A schematic diagram showing a wing-like drilling-induced fracture. The fracture length is given as *L*. The *x*-directed transmitter makes an angle θ to the *x*-axis.

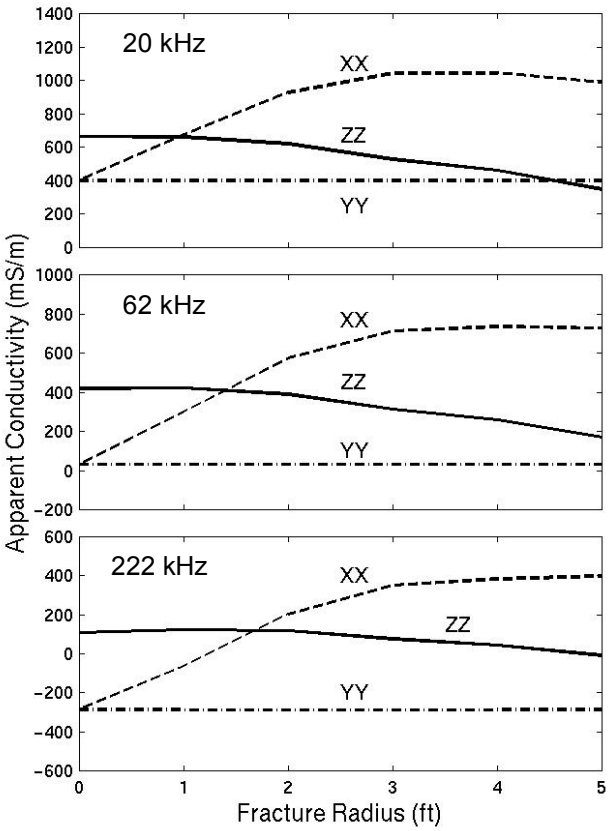


Figure 2. The synthetic XX, YY, and ZZ logs as a function of the fracture length. Note that the XX log has a larger sensitivity to the fracture length than the conventional coaxial (ZZ) log.

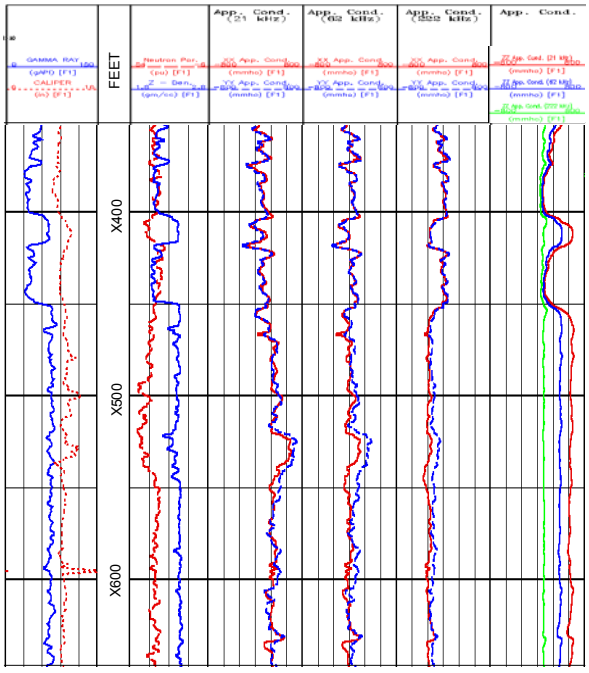


Figure 3. The XX, YY, and ZZ apparent conductivities (the last four tracks). Notice that the XX and YY logs are indiscernible above X460 ft and show significant differences between X510 and X560 ft.

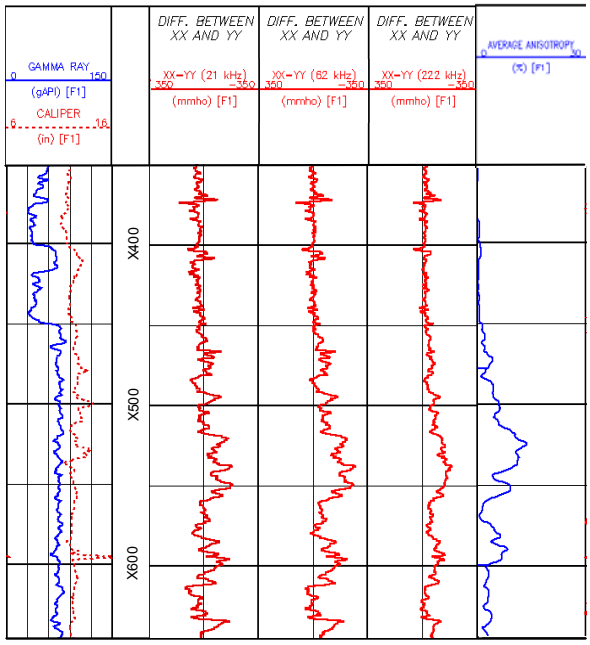


Figure 4. The differences between the XX and YY apparent conductivities shown in Figure 3. The maximum difference occurs between X520 ft and X560 ft.

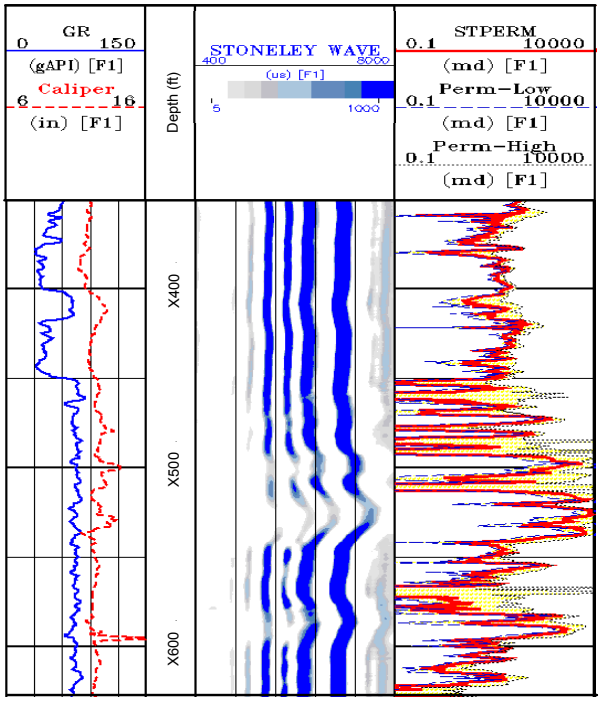


Figure 5. The Stoneley waveforms and the formation permeability derived from the Stoneley logs. Notice that the permeability in the interval of X520–540 ft is about two orders of magnitude higher than that of the upper portion of the well interval that contains porous sands.

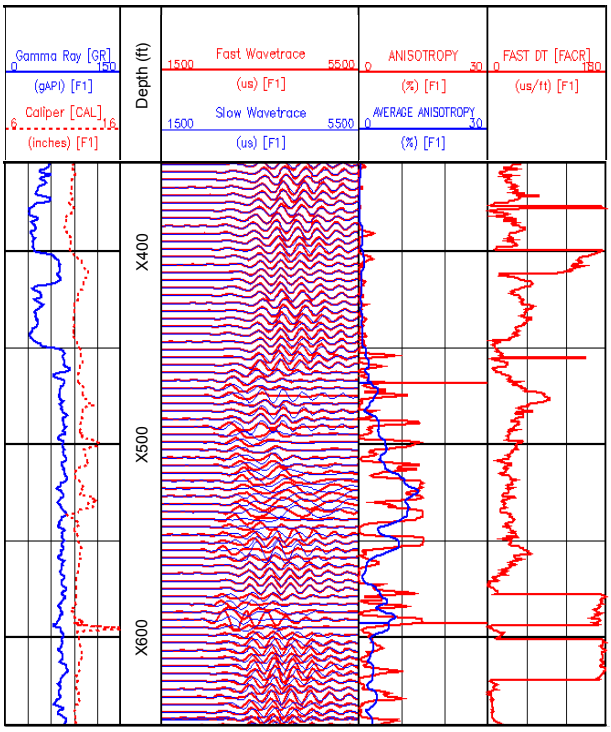


Figure 6. The crossed-dipole acoustic waveforms show shear wave splitting below X450 ft, especially in the interval of X490–550 ft. The azimuthal anisotropy ratio derived from the fast and slow shear waves reaches about 14% around X525 ft. The fast shear azimuth angle (last track) between X500 and X550 ft is about 30°.

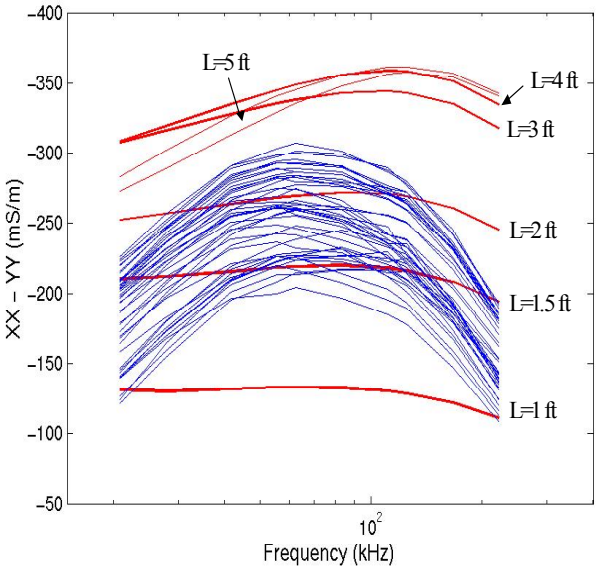


Figure 7. The differences between the measured XX and YY logs (blue lines) superimposed on the theoretically predicted differences between the two (red lines). The measured data are selected from the depths intervals around X535 ft and X550 ft, corresponding to the maximum differences between the XX and YY logs. The fracture lengths in this intervals are estimated to be around 1.5–2 ft.